

# Intelligent Power Management of Islanded DC Microgrid based on Droop Fuzzy Control

Mehrdad Beykverdi<sup>1</sup>, Abolfazl Jalilvand<sup>2</sup>, Mehdi Ehsan<sup>3</sup>

<sup>1</sup>Department of Electrical Engineering, Science and Research branch, Islamic Azad University, Tehran, Iran

<sup>2</sup>Department of Electrical Engineering, University of Zanjan, Zanjan, Iran

<sup>3</sup>Department of Electrical Engineering, Sharif University of Technology, Tehran, Iran

**Abstract**— This paper presents a new intelligent control strategy for DC microgrid in islanded operation mode based on droop control method. The DC microgrid under study included a Wind Turbine Generator (WTG), photovoltaic (PV), battery energy storage system (BESS) and a linear resistive load. According to the proposed method, each of distributed generation (DG) sources and BESS can be deployed independently within any controlled microgrid through the fuzzy control strategy. Proposed fuzzy control regulated virtual resistance of DGs and BESS unit locally and real-time based on the available power of DGs and the battery state of charge (SOC), to coordinate the module performances independently and establish the power balance and regulating DC bus voltage. Proposed control strategy for BESS enables the microgrid to supply independently the power required for the load demand when the DGs are not capable of supplying the required power to the load. The proposed fuzzy control strategy was applied locally and without dependency on the telecommunication links or any centralized energy management system. In order to validate the proposed method, the control system was implemented on a DC microgrid within MATLAB/SIMULINK, where the simulation results were analyzed and validated.

**Keywords**—DC microgrid, fuzzy inference system (FIS), droop method, decentralized control, islanded operation.

## I. INTRODUCTION

Microgrid refers to an integration of loads and distributed generation sources in low or medium voltage levels functioning as a power system for power generation and, if possible, as combined heat and power (CHP) [1–4]. A microgrid is utilized through two modes of connected or independently of the network. Electrical energy generation sources used in microgrids can be micro-turbines, fuel cells, Photovoltaic (PV) solar cells, Wind Turbine Generator (WTG) or other forms of distributed generation along with any storage devices such as super-capacitors and batteries [5,6]. With the progress made in distributed generation technology, there have been many advantages together with numerous problems in terms of network operation and

protection. For example, one of the problems arising due to the growth and development of power systems is the aggravated level of fault current and short circuit because of the presence of Distributed Generations (DG). In addition, it is crucial to coordinate DG and Battery Energy Storage System (BESS) units in order to avoid that the power generated by DG may collapse the system when BESS are full of the charge and there is a power unbalance in the microgrid. So, DGs may change their control strategies from MPPT<sup>1</sup> to a control strategy for regulating the voltage on the DC bus [7,8]. A good stored energy balance has been achieved, by adaptively adjusting the virtual resistance in droop controllers [9]. However, a centralized supervisory control is used, and there is a single point of failure in the system. Additionally, the voltage regulation is not strongly guaranteed.

The power electronic interfacing converter control is a very important issue in the operation of a DC microgrid, particularly for the load sharing between different units. Various control methods have been proposed to achieve efficient power sharing in a parallel converter system, such as master–slave control, and circular current-chain (3C) control, among others. To satisfy the requirements of a distributed configuration, droop control without communication is commonly accepted as a proper power sharing method in a microgrid. In a droop-controlled DC microgrid, the power sharing method is realized by linearly reducing the voltage reference as the output current increases. Although droop control is widely employed as a decentralized method for load power sharing, its limitations should be noted. The output current sharing accuracy is degraded due to the effect of the voltage drop across the line resistance [10]. In addition, a voltage deviation is produced when droop control is realized by reducing the DC output voltage. To overcome this problem, a decentralized secondary controller was proposed to eliminate the voltage deviation [10]. This method was useful for restoring the DC bus voltage, while the effect of the enhancement of current sharing accuracy was not

<sup>1</sup> Maximum Power Point Tracking

obvious enough. The main purpose of analyzing the microgrid for power management is to maintain power balance between DGs and BESS, DC bus voltage regulation and minimizing power losses in the system concurrently [11]. Although the mentioned targets can be achieved by centralized controllers, implementation of the above method requires high-speed communication links, which reduce the reliability of the system [12]. It is noteworthy that functional status of the microgrid is identified and analyzed by DC voltage and transition between different microgrid operating points. In [13], four-terminal DC microgrid with a voltage source converter connected to the main network involves a WTG, a BESS and a linear DC load. In independent and local decentralized microgrid control, the virtual resistance value is determined by trial and error, or artificial intelligence techniques, where the former is extremely time-consuming and rarely yields an optimal solution [14]. When microgrid operates in island mode, DG converter operates as voltage source playing the role of slack bus in the conventional power system [15,16]. Given the optimal allocation of power between DG units, the controlling effect on the circulating currents among resources is necessary to reduce power losses. In addition, coordination of DG and BESS units are necessary to control of battery charge and discharge process. In this case, the DG may change their control strategy from MPPT to a control strategy for regulating the voltage on the DC bus. Moreover, the most effective solution of charging a BESS is by means of a two stage procedure which involves two different control loops [17,18]. Given the above points, the operation of each DG and BESS in the microgrid should be accompanied by a decision-maker strategy to switch between controllers. Conventional droop methods lead to weak current sharing and voltage drop in DC microgrid [19]. The circulating current in the microgrid is created due to the mismatch of output voltage of power converters. Therefore, this reference introduced an indicator named Droop Index (DI), which both improves microgrid performance and reduces losses and current allocation difference in the converter output. The proposed adaptive droop method in mentioned reference and also, in [20] can curtail the circulating current and current allocation difference of converters by adaptive virtual resistance.

In this paper and after the introduction part, configuration of the proposed DC microgrid is presented in section 2. In section 3, the FIS control system application for adjusting virtual resistance in DGs and BESS unit is demonstrated and section 4 shows the simulation results and the validation of the control system. At the last part, conclusion of the investigation is explained.

The main contributions of this investigation are: maintaining of power balance, voltage regulation and

keeping state of charge (SOC) of battery in allowable range concurrently. The adaptive I/V characteristic curve is regulated locally and real-time based on the available power of DGs, load demand and battery SOC, so as to achieve decentralized control in the microgrid. Also, BESS undertakes supplying the load demand only in a mode where the load demand is more than the total generation power of DGs. At this point, the BESS supplies the power load shortage based on the SOC, until it reached to minimum SOC. The control strategies for each module within the microgrid were implemented through multi-loop fuzzy control without using communication links or central energy management system.

## II. CONFIGURATION OF DC MICROGRID

Application of a DC microgrid can improve stability, reduce losses and enhance the flexibility of the power system. Generally, the microgrids entail several advantages including: greater energy efficiency, lower costs of generation and transmission and reduced greenhouse gas emissions. As opposed to the AC microgrids, the DC microgrids inherently entail certain advantages such as simplicity in control system design, since there is no need to control the frequency. Microgrids design and control can decrease the number of stages involved in DC power electronic conversion and curtail the switching losses. Moreover, DC systems will not face challenges such as harmonics and inrush current of power transformers. The advantages of the DC microgrid over the conventional AC microgrids can be categorized as follows [21]:

1. More than 90% of household loads can be directly fed by the DC power; such as the devices based on microprocessors, PC power supplies, switching power supplies, electronic ballasts for fluorescent lighting, LED lights and variable frequency drives in heating, cooling and ventilation systems.
2. The DC power can maximize the generation power through sources such as PV and fuel cell in order to prevent the power conversion losses (eliminating one or two stages of power conversion, absence of reactive power and harmonics). In conventional AC systems, the energy generated by PV is converted to AC and is converted again to the DC power in another stage for some consumers.
3. The DC power can effectively adapt with energy storage systems and enhancing the efficiency of the system. Moreover, it is widely applied in hybrid vehicles.
4. There is no need to coordinate the energy generation sources within the DC microgrid.
5. Loads are not affected by frequency deviations, three-phase voltage imbalance or voltage harmonics.

6. Inrush current and single phase generators have no impact on the power quality.

Figure 1 illustrates the block diagram of the proposed DC microgrid. In the mentioned figure, the first module is PV, the second one is WTG and the third module is the BESS. The PV module is connected to DC bus by a DC-DC converter as the droop control strategies are adopted on this converter where the switching is controlled through the PWM method. Since the WTG has a three-phase AC output, it is first converted by a full-wave rectifier into DC output applied on a DC-DC converter based on droop control strategy. Also, in order to simplify calculations and having a general rule, the dynamics of WTG are disregarded. Similar to the PV module, the BESS is connected to the microgrid common bus by a DC-DC power electronics converter, controlling the BESS charging and discharging process. The microgrid load was supposed

to be resistive linear load, to evaluate the microgrid control strategies by decreasing or increasing level of load demand. It is very important to coordinate performance of DGs and BESS units in order to avoid that the power generated by DGs may collapse the system, when BESS are full and there is a power unbalance in the microgrid. In this view, the DGs may change their control strategy from maximum power point tracking (MPPT) to a control strategy for regulating the voltage on the DC common bus. The proposed microgrid is generally formed around 48V common bus, these kinds of low voltage microgrids have been widely used for residential and communication applications. In particular, the microgrid will be simulated under islanded operation mode since this mode is so important for remote applications, and the interaction of BESS with DGs plays an important role.

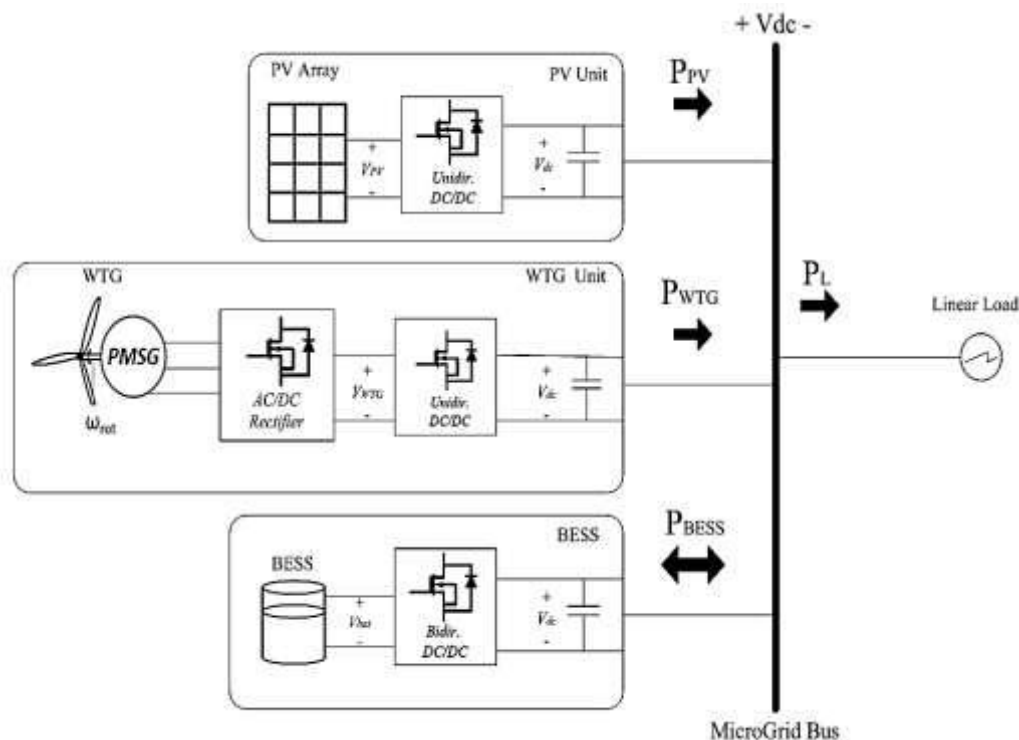


Fig.1: Block diagram of proposed DC microgrid

When the DC microgrid operates in islanded mode, it is easy to identify two different operation modes based on the kind of DGs responsible for the DC common bus regulation. In other words, the DC common bus voltage can be regulated by BESS (mode I) or by DGs (mode II). Also, the control strategy that manages BESS, changes in accordance to the SOC of the BESS and the balance between the power generated by the DGs and the load demand. In the case of the DG, the control strategy changes in accordance to the voltage in the common DC bus in the same way that changes the operation mode of the microgrid. As a consequence, each distributed energy resource (DER) including BESS and DGs requires at least

two inner control loops in order to operate under the two different operation modes and control conditions. Figure 2 shows transition diagram between operation modes in DC microgrid. According to this figure, in state 1 DGs are in MPPT mode and deliver maximum generation power based on their capacity and BESS is in voltage droop control mode to regulate DC bus voltage. If the voltage of DC bus is 5% greater than reference value, the controller switches to state 2 that DGs are in voltage droop mode and battery is under constant voltage charger condition to absorb excess power of the microgrid.

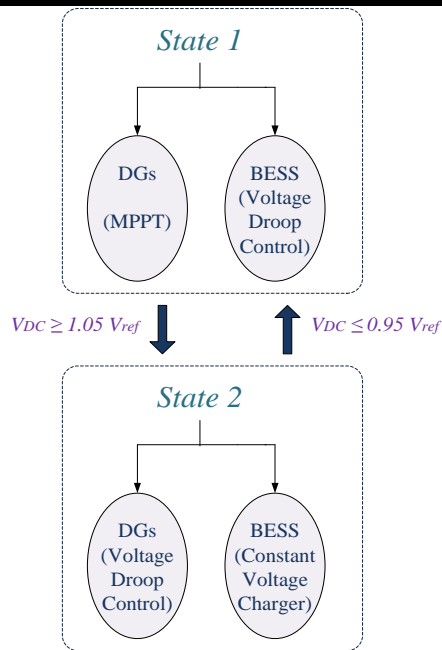


Fig.2: Transition diagram between operation modes

In the mode 1, both DGs operate under MPPT and they can be supposed as a constant power source (CPS). Meanwhile, the converter of the BESS operates under voltage droop control and it is responsible for regulating the DC bus voltage. In fact, a CPS can be represented by a resistor in parallel to a constant current source, and the voltage source in series with the resistance ( $R_d$ ) represents a battery operating under voltage droop control. When the voltage of BESS reaches the reference value ( $V_{float}$ ), the control of converter switches to a constant voltage charger for the BESS, in which, the BESS absorbs as much current as needed to keep its voltage at  $V_{float}$ . When BESS reaches the float voltage, the DGs continue operating in MPPT mode, until a voltage threshold is reached in the DC bus. Then, the DGs change their inner control loops from MPPT to a voltage droop control in which the power injected from the DGs are limited to the load demand of the microgrid. At this moment, the microgrid is under operation mode II. In the mode 2, the DGs are responsible for DC common bus regulation, since BESS is under constant voltage charge. For that reason, the BESS will only take as much current as necessary from the microgrid for keeping the BESS voltage regulated at  $V_{float}$ . The DC microgrid continues operating in this mode until a voltage threshold ( $V_L$ ) is reached at the DC bus. This may occur whether load demand is bigger than the generation power of DGs. At this point, the DC microgrid changes to operation mode 1 again. The following section is focused on representing the voltage droop controllers and fuzzy adjustment of virtual resistance.

### III. FIS APPLICATION FOR ADJUSTING VIRTUAL RESISTANCE

The main objective for design of fuzzy inference system (FIS) for adjusting virtual resistances is establishing power balance in the DC microgrid, and consequently avoids deep charge or discharge of the battery. Also, another control objective is in order to reduce the voltage deviation in the common DC bus. Finally, the proposed strategy is designed to be decentralized, since only local variables are to be used for performing the adjustment of  $R_d$ . Consider that voltage droop controllers are used by BESS and DGs at different operational modes of the microgrid, a different fuzzy controller may be designed for BESS and DGs. When battery is in the process of charge and discharge, the power balance is managed by droop control loops. Therefore, the output voltage is given by the following equation:

$$V_{DC} = V_{ref} - I_L \cdot R_d \quad (1)$$

Where  $R_d$  is the virtual resistance at each droop control loop,  $V_{DC}$  is the voltage at the common DC bus,  $V_{ref}$  is the voltage reference and  $I_L$  is the output current at each DC/DC converter [21]. It's necessary to mention that a FIS can summarize all the qualitative knowledge, explained above. Hence, a fuzzy controller can deal with different control objectives at the same time which is, in this particular case, stored energy balance and reduction of dc bus voltage deviation. In fact, a FIS can use the experience and the knowledge of an expert about the expected behavior of the system in order to work out the virtual resistance at each control loop.

$$V_{err} = V_{ref} - V_{DC} \quad (2)$$

$$SOC = SOC(0) - \int_0^t \frac{I_{bat}(\alpha)}{C_{bat}} d\alpha \quad (3)$$

According to the above points, a Sugeno FIS has been proposed for adjusting the  $R_d$  at each battery converter system. The FIS uses the SoC and the voltage error ( $V_{err}$ ) expressed in (2) as the inputs, and the virtual resistance  $R_d$  as the output to adjust virtual resistance of the BESS unit. The SOC is estimated by ampere-hour (Ah) counting method expressed in (3), Where  $SOC(0)$  represents the initial SoC,  $C_{bat}$  is the capacity of the BESS and  $I_{bat}$  is the current of the BESS. Figure 3 shows the diagram of the fuzzy controller used for the adjustment of the  $R_d$  of battery. In other words, the fuzzy control is only used under operation mode I, when the battery is under voltage droop control in State 1. The advantages of proposed fuzzy control system for the BESS unit are increasing the life of battery cells, controlling the SOC in allowable range and using the BESS unit as a backup unit for the DC microgrid.

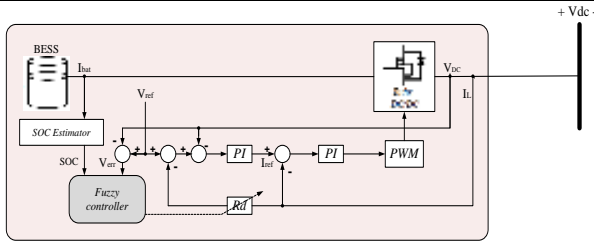


Fig.3: Control diagram of fuzzy system for BESS

The major advantages of fuzzy logic system implementation for battery monitoring system are the accuracy and efficiency of FIS system. Based on the abilities of this method, it can be monitored the battery SOC real-time and avoiding over-charge or deep-charge of the BESS. So, it helps to improve BESS efficiency and increase the cells life time.

Figure 4 shows the control surface of the proposed FIS, which summarizes the behavior of the proposed method, where the virtual resistance is adjusted based on the expected behavior explained of the system and figure 5 shows the Gaussian membership functions of the FIS.

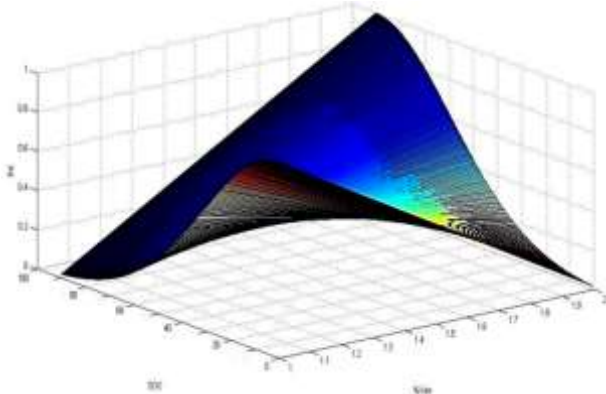


Fig.4: Control surface of the FIS

Based on the above figure, the inputs for the fuzzy control system in the BESS units are SOC (in the range of 0 and 100 percent) and error voltage (between 1 to 2 percent) and the output is virtual resistance amplitude between 0 to 1 ohm. So, with the variation of the error voltage and SOC of the BESS unit, output  $R_d$  will be changed to inject or absorb the power from the DC common bus.

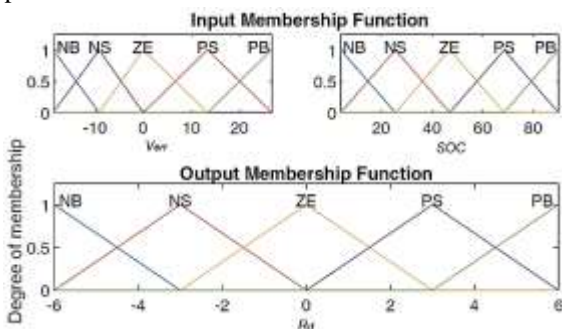


Fig.5: Membership function of FIS for BESS

The FIS will work towards the objective of minimizing variation in the DC microgrid while satisfying all the constraint. A total of 25 rules are set based on expert knowledge and shown in Table 1 based on Mamdani FIS. The 5 membership function of Table 1 represents the output of  $R_d$ . Where N, P, B, S and ZE represents Negative, Positive, Big, Small and Zero respectively.

Table.1: Fuzzy rules for BESS

$R_d$		$V_{err}$				
		NB	NS	ZE	PS	PB
SOC	NB	PB	PS	ZE	ZE	ZE
	NS	PB	PS	ZE	NS	NS
	ZE	PS	PS	ZE	NS	NS
	PS	PS	PS	ZE	NS	NB
	PB	ZE	ZE	ZE	NS	NB

Furthermore, the range of the output ( $R_d$ ) in the FIS can be established by analyzing the equivalent circuit of Fig. 1, where a general expression for a general number of BESS and DG operating in MPPT may be expressed as shown in the following equation:

$$V_{DC} = \frac{V_{ref} + I_{CPS}}{\frac{1}{R_{deq}} + \frac{1}{R_{load}} + \frac{1}{R_{CPS}}} \tag{4}$$

Where  $R_{deq}$  and  $R_{CPS}$  are the equivalent virtual resistance and the equivalent resistant of the DG, seen as constant power source, respectively.  $I_{CPS}$  is the equivalent current of the constant power source.  $R_{CPS}$  and  $I_{CPS}$  can be well approximated by:

$$R_{CPS} \approx \frac{V_{DC}^2}{P_{CPS}} \tag{5}$$

$$I_{CPS} \approx 2 \frac{P_{CPS}}{V_{DC}} \tag{6}$$

Where  $P_{CPS}$  is the total power generated by DG. By replacing (5) and (6) in (4) it is possible to obtain the following equation:

$$V_{DC} \left( \frac{1}{R_{deq}} + \frac{1}{R_{load}} \right) - P_{CPS} \frac{V_{ref}}{R_{deq}} = 0 \tag{7}$$

From (7) gives a solution for the common DC voltage:

$$V_{DC} = \frac{V_{ref} + \sqrt{\left( \frac{V_{ref}}{R_{deq}} \right)^2 + 4P_{CPS} \left( \frac{1}{R_{deq}} + \frac{1}{R_{load}} \right)}}{2 \left( \frac{1}{R_{deq}} + \frac{1}{R_{load}} \right)} \tag{8}$$

Where the value of the power generated by DG is taken as positive. Thus, just the positive solution is viable in this case, since the voltage of the common DC bus has to be

positive. Then, when a maximum voltage deviation is defined, it is possible to solve (8) in order to determine the maximum and minimum value for virtual resistance ( $R_d$ ). When the system operates under operation mode II, the DGs are responsible for DC bus voltage regulation. At this point, both DGs are operating under droop control loops (state2). Similarly, the  $R_d$  at each unit can be adjusted for reducing the voltage deviation. For that reason, an iterative adjustment of the virtual resistance has been proposed for obtaining good voltage regulation as well as suitable power sharing at the same time to establish power balance in the system. The adjustment of  $R_d$  is based on a FIS of which output is an incremental signal. Then, depending on the voltage error ( $V_{err}$ ), the virtual resistance will be increased or decreased. Figure 6 shows the diagram of the control loop used for the adjustment of  $R_d$  at each DG unit. At this point, the microgrid is under operation mode II and the control loops are in state 2. The controller comprises a FIS and an integrator to get desired value of the virtual resistance.

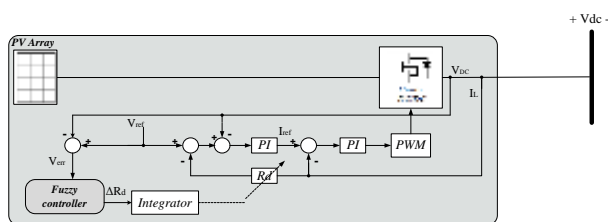


Fig.6: Control diagram of fuzzy system for PV unit

IV. SIMULATION RESULTS

A DC microgrid composed of DG units of PV and WTG and BESS was simulated within MATLAB/SIMULINK so as to evaluate the performance of the proposed control strategy, and also, table 2 shows the microgrid parameters. Performance of the proposed fuzzy control system was assessed through changing in load demand level. In the first scenario, the performance of DC microgrid control strategy

was evaluated in response to 250 W of load. Then, the microgrid behavior was analyzed in 350 W of load demand in the second scenario; that the simulation results in both scenarios are compared with fixed virtual resistance and fuzzy-based virtual resistance adjustment.

Table.2: DC microgrid parameters

Parameter	Symbol	Value
DC bus voltage reference	$V_{ref}$	48V
Max. power from RES	$P_{max}$	300w
Max. power in the load	$P_{Loadmax}$	250 – 350 w
Float voltage	$V_{float}$	54V
Nominal virtual resistance	$R_{d-nom}$	0.7 Ω
Low voltage threshold	$V_L$	45.6V
High voltage threshold	$V_H$	50.4V
Nominal battery capacity	$C_{bat}$	2 Ah
Minimum SOC	$SOC_{min}$	% 40
Maximum SOC	$SOC_{max}$	% 90
Initial SOC	$SOC_{in}$	% 60

Figure 7 illustrates the simulation results of DC microgrid under 250 W load demand with fixed virtual resistance. In the first part of the mentioned figure, output or delivered power of the DGs are shown. At  $t=1^s$ , a 250 W load demand is connected to DC common bus and the changes in the level of generation power is displayed. Although the load demand is 250 W and it is 50 W less than generation capacity of the DGs, but BESS started to discharge because of the droop characteristics of the unit with fixed slope or fixed virtual resistance. Second part of the graph, shows the voltage variation of the common bus. At first, the voltage is 54 V and after  $t=1^s$  with load switching, the amplitude is decreased and stabled on the 50 V, that is in allowable range. Third part of the mentioned graph illustrates the delivered or generated current of the PV and WTG unit.

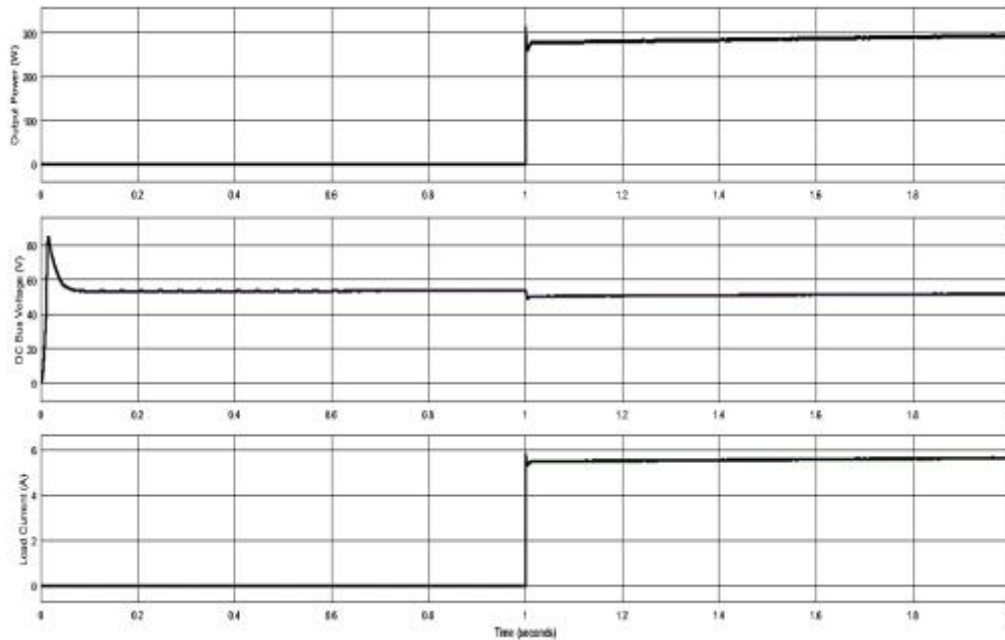


Fig.7: Simulation results of DC microgrid under 250 W load demand with fixed virtual resistance: a) Output power of DGs (w), b) DC bus voltage (v), c) Load current (A)

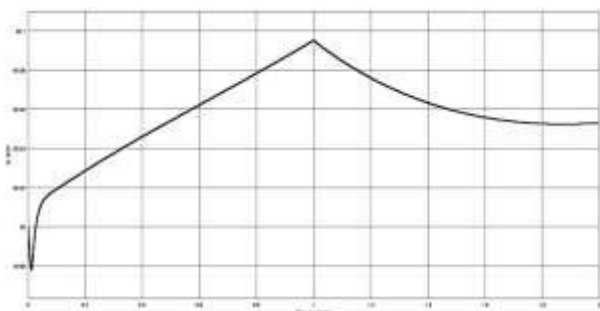


Fig.8: Battery SOC under 250 W load demand with fixed virtual resistance

Figure 8 shows the battery SOC under 250 W load demand with fixed virtual resistance. As illustrated, battery is charged before load switching. After  $t=1s$ , SOC is decreased for some while, but after that, discharging process is stopped and battery will be in floating or charging mode according to the available power of the microgrid. It's necessary to say that based on the available power and MPPT mode of DGs, the BESS in Charged until 90%. After this point, battery will be in floating mode and charging process stopped.

Figure 9 displays the simulation results of DC microgrid under 350 W load demand with fixed virtual resistance. In the first part of the mentioned figure, output power or delivered power to microgrid is shown. At  $t=1s$ , 350W load

demand is connected to common DC bus and the changes in the level of generation power is displayed. In fact, the load demand is 350 W and it is 50 W more than generation capacity of all DGs. So, BESS started to discharge to supply power shortage (50 W) and establish power balance in the DC microgrid based on droop characteristics of the unit with fixed virtual resistance. In this scenario, DGs delivered maximum generation power and they can be supposed as constant power sources. In addition, BESS acts as a backup unit in the microgrid to support the load demand and avoiding load shedding. Second part of the figure shows the voltage variation of the common bus. At first, the voltage is 54 V and after  $t=1s$  with load connecting to the microgrid, the voltage is decreased and stabled on the 47 V, that is the low voltage threshold. Also, there is a lot of variations in DC bus voltage because of fixed virtual resistance that cause more reduce in voltage amplitude with simulation time increasing based droop characteristics. In this condition, if the load will be increased more and SOC decreased to 40%, hence the DC bus voltage decreased to below of the allowable range and load shedding strategy should be performed, that is out of the scope of this investigation. Third part of the mentioned graph illustrates the delivered current of the PV and WTG units. Generally, after the load switching DGs started to deliver power to the microgrid and supplied load demand.

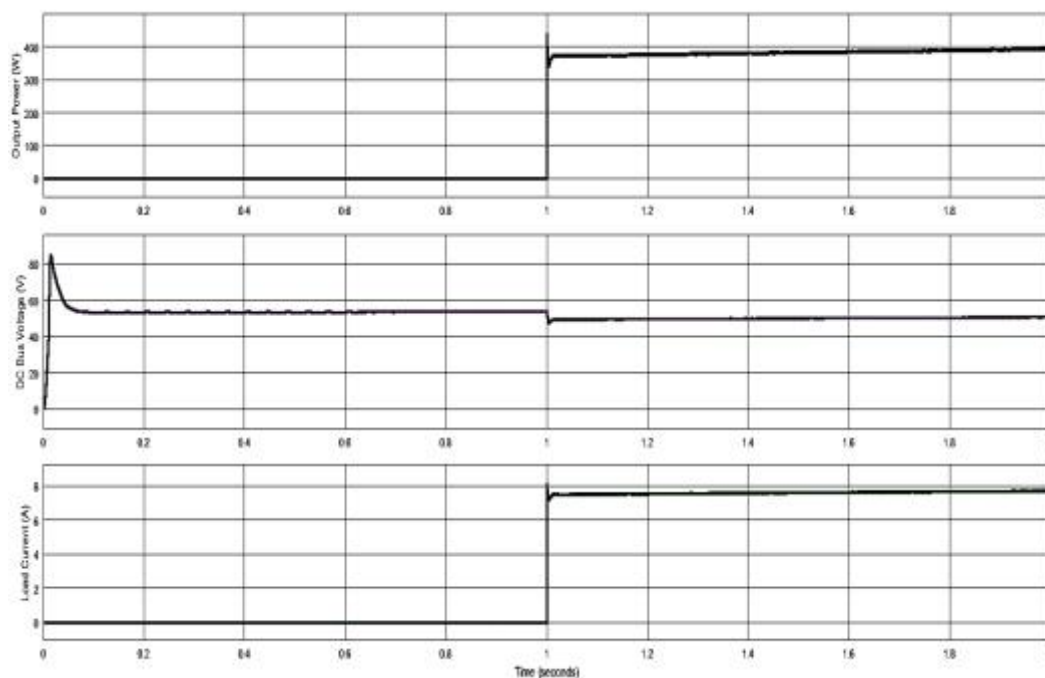


Fig.9: Simulation results of DC microgrid under 350 W load demand with fixed virtual resistance: a) Output power of DGs (w), b) DC bus voltage (v), c) Load current (A)

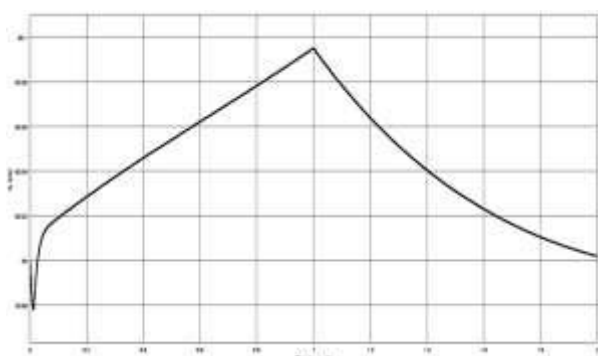


Fig.10: Battery SOC under 350 W load demand fixed virtual resistance

Figure 10 shows the BESS SOC under 350W load demand with fixed virtual resistance. As illustrated, battery is discharged to supply power shortage and regulate DC bus voltage. After  $t=1^s$  and with load switching, SOC is decreased and after 2 seconds, it reached to initial SOC and continue to decreasing until the minimum SOC.

Figure 11 shows simulation results of DC microgrid under 250 W load demand with proposed fuzzy-based virtual

resistance. In the first part of the mentioned figure, output power or delivered power of the microgrid is shown. At  $t=1^s$ , a 250W load demand is connected to common bus and the changes in the level of generation power is displayed. In fact the load demand is 250 W and it is 50 W less than generation capacity of the DGs, hence BESS started to charge to supply to improve SOC level until 90% according to the MPPT mode of DGs based on droop characteristics of the unit with proposed fuzzy-based virtual resistance. As shown in this figure, power sharing is improved in comparison with the fixed virtual resistance and the generation power is adapted with the load demand exactly. Second part of the graph, shows the voltage variation of the common bus. At first, the voltage is 54 V and after  $t=1^s$  with load switching, the amplitude is decreased a little and stabled on the 52 V that is in allowable range and reached good voltage regulation. As shown, there is less voltage deviation in comparison with the fixed virtual resistance. Third part of the mentioned graph illustrates the delivered or generated current of the PV and WTG units.



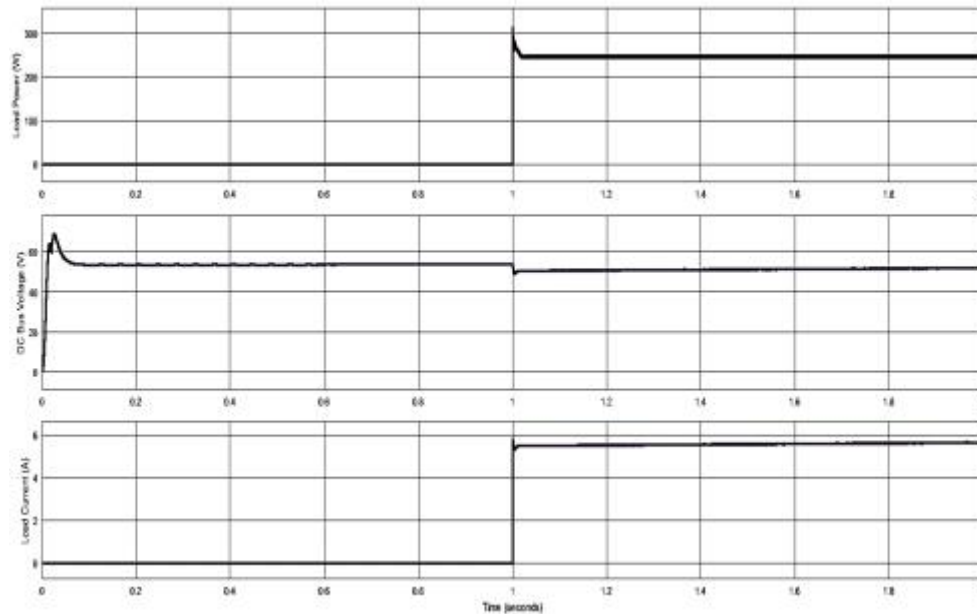


Fig.11: Simulation results of DC microgrid under 250 W load demand with proposed fuzzy-based virtual resistance: a) Output power of DGs (w), b) DC bus voltage (v), c) Load current (A)

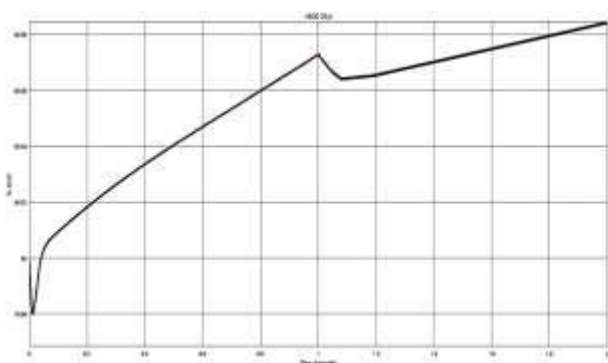


Fig.12: Battery SOC under 250 W load demand proposed fuzzy-based virtual resistance

Figure 12 shows the BESS SOC under 250 W load demand with proposed fuzzy-based virtual resistance. As illustrated, battery is in charging mode, because of available power of microgrid, before load switching. After  $t=1^s$ , SOC is decreased for some while, but after very short time, discharging process is stopped and battery will be in charging mode again, according to the generation power of the DGs. It's necessary to say that based on available power and MPPT mode of DGs, the BESS will be in Charging mode until the SOC reached 90%. After this point, battery will be in floating mode and charging process is stopped to protect the BESS from over charging event. It's obvious that in contrast with fixed virtual resistance mode, the performance of the BESS is improved and it stores excess energy of the system to increase SOC level instantly.

Figure 13 illustrates the simulation results of DC microgrid under 350 W load demand with proposed fuzzy-based virtual resistance. In the first part of the mentioned figure, output power or delivered power the microgrid is shown. At  $t=1^s$ , a 350 W constant power load is connected to common bus and the changes in the level of generation power is displayed. In fact the load demand is 350 W and it is 50 W more than generation capacity of the DGs, hence BESS started to discharge to supply power shortage and make power balance in the DC microgrid based on the droop characteristics of the unit with proposed fuzzy-based virtual resistance. In this scenario, DGs are in MPPT mode and they can be supposed as constant power sources. Also it can be seen that power sharing in this mode is improved and generation power is exactly adapted to the load demand, that 300 W generation power belongs to DGs and 50 W power shortage is supplied by BESS. Second part of the graph, shows the voltage variation of the common bus. At first, the voltage is 54 V and after  $t=1^s$  with load switching, the amplitude is decreased a little and stabled on the 50 V that is more than fixed virtual resistance result in previous mode. In this condition, if the load be connected more and SOC decreased to 40%, hence load shedding strategy should be performed, that is out of the scope of this paper. Third part of the mentioned graph illustrates the delivered or generated current of the PV and WTG units.

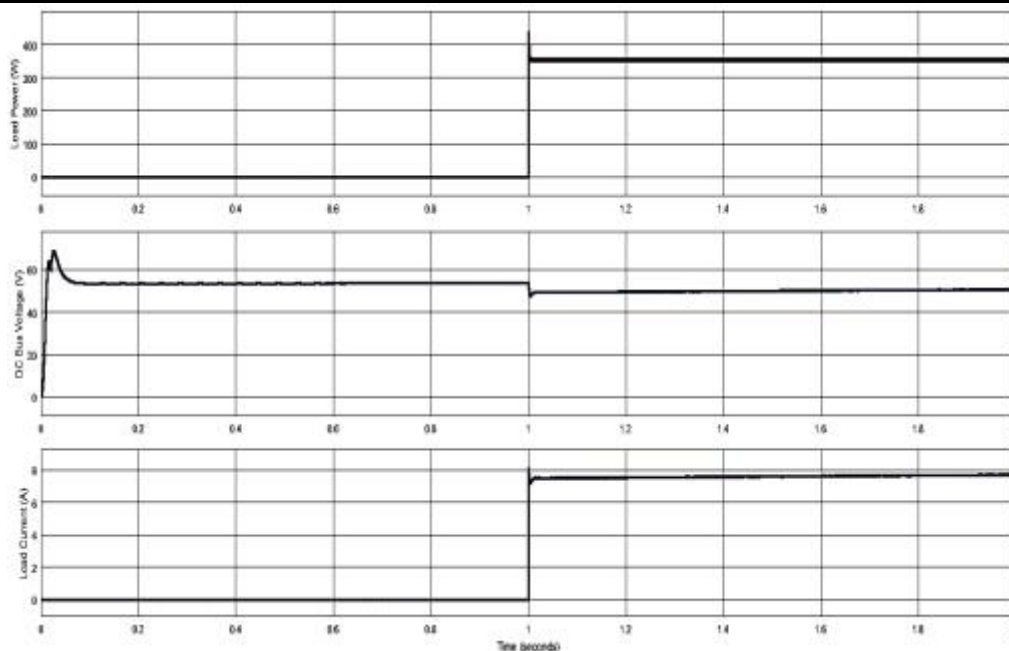


Fig.13: Simulation results of DC microgrid under 350 W load demand with proposed fuzzy-based virtual resistance ( $R_a$ ): a) Output power of DGs (w), b) DC bus voltage (v), c) Load current (A)

Figure 14 shows the battery SOC under 350 W load demand with proposed fuzzy-based virtual resistance. As illustrated, battery is started to discharge to supply power shortage and regulate DC bus voltage and establish power balance in the microgrid. According to the last scenario, BESS is charged until the SOC of 80%. After  $t=1^s$  and with load switching, SOC of battery started to decrease, and in this mode and with fuzzy adjusting virtual resistance, the rate of discharging is faster in comparison with the fixed virtual resistance to adapt load demand. Discharging process in continued until the minimum level of SOC.

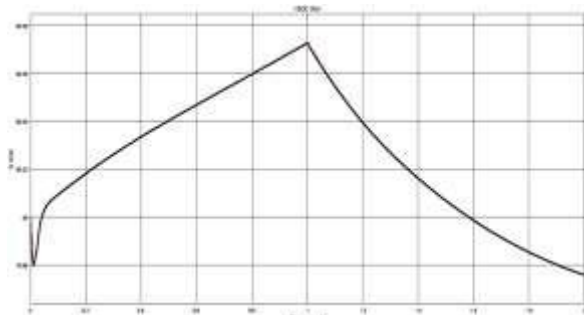


Fig.14: Battery SOC under 350 W load demand proposed fuzzy-based virtual resistance

## V. CONCLUSION

This paper proposed an intelligent adjustment of the virtual resistance by using fuzzy inference system that assures suitable storage energy in BESS and low voltage deviations. Also this method is expandable and it's not required centralized control or central energy management system. The proposed decentralized technique regulates

virtual resistance to control power generation of DGs based on droop characteristic and SOC level of the BESS, so as to supply the load demand or recharge the battery. The outcome is that power can be injected into the DC microgrid when the load has exceeded the total generation capacity of DGs. Moreover, the BESS is integrated into the microgrid either in charge or floating modes based on the SOC and the conditions of generation and consumption. In fact steady state error is always desired in DC bus, since the DC bus voltage is used for bus signaling. Generally the fuzzy method proposed in this paper has shown its advantages in dealing with different control objectives. Additionally proposed FIS method can be scaled to different values of virtual resistances. The proposed fuzzy control strategy can add to the microgrid any number of DG units or batteries without violating or interfering with the generalities offered. Hence, the proposed strategy can enhance the efficiency and flexibility of DC microgrids. The proposed intelligent decentralized control scheme was evaluated and validated through simulation in MATLAB/SIMULINK.

## REFERENCES

- [1] B. Patterson, "DC come home: DC microgrids and the birth of the Enernet", *IEEE Power Energy Mag.*, vol. 10, no. 6, pp. 60-69, 2012.
- [2] A. Kahrobaeian, Y. Ibrahim Mohamed, "Network-Based hybrid distributed power sharing and control for islanded microgrid systems", *IEEE Trans. Power Electron.*, vol. 30, issue 2, pp. 603-617, 2015.

- [3] S. Anand, B. Fernandes, M. Guerrero, "Distributed control to ensure proportional load sharing and improve voltage regulation in low voltage DC microgrids", *IEEE Trans. Power Electron.*, vol. 28, issue 4, pp. 1900-1913, 2013.
- [4] Z. Zeng, H. Yang, S. Tang, R. Zhao, "Objective-Oriented power quality compensation of multifunctional grid-tied inverters and its application in microgrids", *IEEE Trans. Power Electron.*, vol. 30, issue 3, pp. 1255-1265, 2015.
- [5] Wei Du, Q. Jiang, M. Erikson, R. Lasseter, "Voltage-Source control of PV inverter in a CERTS microgrid", *IEEE Trans. Power Delivery*, vol. 29, issue 4, pp. 1726-1734, 2014.
- [6] Liang Che, M. Shahidehpour, "DC microgrids: Economic operation and enhancement of resilience by hierarchical control", *IEEE Trans. Smart Grid*, vol. 5, issue 5, pp. 2517-2526, 2014.
- [7] R. Majumder, "A hybrid microgrid with DC connection at back to back converters", *IEEE Trans. Smart Grid*, vol. 5, issue 1, pp. 251-259, 2014.
- [8] B. Wang, M. Sechilariu, F. Locment, "Intelligent DC microgrid with smart grid communications: Control strategy consideration and design", *IEEE Trans. Smart Grid*, vol. 3, no. 4, pp. 2148-2156, 2012.
- [9] P.C. Loh, D. Li, Y.K. Chai, F. Blaabjerg, "Autonomous control of interlinking converter with energy storage in hybrid AC-DC microgrid", *IEEE Trans. Industry Applications*, vol. 49, issue 3, pp. 1374-1382, 2013.
- [10] Chi Jin, Peng Wang, J. Xiao, Yi Tang, F.H. Choo, "Implementation of hierarchical control in DC microgrids", *IEEE Trans. Industrial Electronics*, vol. 61, issue 8, pp. 4032-4042, 2014.
- [11] Q. Shafiee, T. Dragicevic, J. Vasquez, J.M. Guerrero, "Hierarchical control for multiple DC microgrids clusters", *IEEE Trans. Energy Conversion*, vol. 29, issue 4, pp. 922-933, 2014.
- [12] Chi Jin, Peng Wang, J. Xiao, Yi Tang, F.H. Choo, "Implementation of hierarchical control in DC microgrids", *IEEE Trans. Industrial Electronics*, vol. 61, issue 8, pp. 4032-4042, 2014.
- [13] N. Eghtedapour, E. Farjah, "Distributed charge/discharge control of energy storages in a renewable-energy-based DC microgrid", *IET Renew. Power Gener.*, vol. 8, Issue 1, pp. 45-57, 2014.
- [14] T. Caldognetto, P. Tenti, "Microgrids operation based on Master-Slave cooperative control", *IEEE Journal of Emerging and Selected Topics in Power Electronics*, vol. 2, issue 4, pp. 1081-1088, 2014.
- [15] R. Majumder, "A hybrid microgrid with DC connection at back to back converters", in *Proc. IEEE Trans. Smart Grid*, 2013.
- [16] A. Paquette, M. Reno, R. Harley, D. Divan, "Sharing transient loads: Causes of unequal transient load sharing in islanded microgrid operation", *IEEE Industry applications Magazine*, vol. 20, issue 2, pp. 23-34, 2014.
- [17] N. Eghtedapour, E. Farjah, "Power control and management in a hybrid AC/DC microgrid", in *Proc. IEEE Trans. Smart Grid*, 2014.
- [18] L. Che, M. Khodayar, M. Shahidehpour, "Only connect: Microgrids for distribution system restoration", *IEEE Power Energy Mag.*, vol. 12, no. 1, pp. 70-81, 2014.
- [19] X. Lu, K. Sun, J.M. Guerrero, J.C. Vasquez, L. Huang, "State of charge balance using adaptive droop control for distributed energy storage systems in DC micro-grid applications", *IEEE Trans. Industrial Electronics*, vol. 61, issue 6, pp. 2804-2815, 2014.
- [20] S. Augustine, M.K. Mishra, N. Lakshminarasamma, "Adaptive droop control strategy for load sharing and circulating current minimization in low-voltage standalone DC microgrid", *IEEE Trans. Sustainable Energy*, vol. 6, no. 1, pp. 132-141, 2015.
- [21] F. Valencia, D. Saez, J. Collado, F. Avila, A. Marquez, J. Espinosa, "Robust energy management system based on interval fuzzy model", *IEEE Transactions on Control Systems Technology*, vol. 24, issue 1, pp. 140-157, 2016.